

## Influence of water supply on cork increment and quality in *Quercus suber* L.

Ana Patrícia Poeiras<sup>1\*</sup>, Teresa Oliveira<sup>2</sup>, Joana Reis<sup>3</sup>, Peter Surový<sup>4</sup>,  
Maria Emília Silva<sup>5</sup>, Nuno de Almeida Ribeiro<sup>6</sup>

<sup>1</sup> University of Évora, Mediterranean Institute for Agriculture, Environment and Development (MED) & Department of Plant Science, School of Sciences and Technology, Pólo da Mitra, Ap. 94, PT – 7006–554 Évora, Portugal

<sup>2</sup> University of Évora, Mediterranean Institute for Agriculture, Environment and Development (MED) & Veterinary Department, Pólo da Mitra, Apart. 94, PT – 7002–554 Évora, Portugal

<sup>3</sup> Superior School of Agriculture, Polytechnic Institute of Viana do Castelo, Rua D. Mendo Afonso, 147, Refóios do Lima, PT – 4990–706 Ponte de Lima, Portugal

<sup>4</sup> Czech University of Life Sciences Prague, Faculty of Forestry and Wood Science, Department of Forest Management, Kamýčká 129, CZ – 165 00 Praha 6, Suchbátka, Czech Republic

<sup>5</sup> University of Trás-os-Montes e Alto Douro, Department of Forestry Sciences and Landscape Architecture, Quinta de Prados, PT – 5001–801 Vila Real, Portugal

<sup>6</sup> University of Évora, Institute of Earth Sciences (ICT) & Department of Plant Science, School of Sciences and Technology, Pólo da Mitra, Ap. 94, PT – 7006–554 Évora, Portugal

### Abstract

Cork oak (*Quercus suber* L.) grows in the Mediterranean basin including Portugal and is the main species producing cork which is used prevalently in stopper industry. In our paper, cork from *Quercus suber* L. over three consecutive harvests from a traditional rainfed plot, between 1999 and 2017, and cork from an irrigated plot, harvested in 2017, were studied. We applied two X–ray image analysis technologies – X–ray micro-computed tomography and X–ray microdensitometry. Cork development, related with intern porosity, growth and density was studied with the objective of understanding the cork characteristics evolution over the years and with a different water regime. The outcomes of this study suggested an increase in density and porosity over harvests and a slight decrease of the cork growth. Cork samples from the irrigated plot, compared with cork from the same year of extraction in the rainfed plot, showed higher growth rate and higher porosity. The results demonstrated the contribution of climatic factor of precipitation as well as the silviculture model in cork characteristics, showing the relevance of the present work for the definition of the management practices. These may be determinant for enhancing cork quality and quantity production through silviculture measures. Our findings can be particularly useful for stakeholders especially under the conditions of Portugal in terms of increasing the value of the industrial chain of cork.

**Key words:** cork oak; cork characteristics; image analysis; X–ray micro-computed tomography; X–ray microdensitometry

Editor: Bohdan Konôpka

### 1. Introduction

Cork oak (*Quercus suber* L.) is the main species responsible for cork production with sustainable and profitable exploration, growing in the Mediterranean basin. Cork extracted from *Quercus suber* L. is mostly used to the cork stoppers industry (41.6% for natural cork stopper and 28.9% for other types of stoppers (APCOR 2019). Porosity is one of the main characteristics responsible for the type of stoppers developed and is in the basis of industrial classification, also associated to cork growth in

the radial direction and cork density. Porosity is defined as the fraction occupied by lenticular channels and other structural defects (Fortes et al. 2004), which represent macro porosity across the cork profile. The lenticels' grow from the phellogen to the external surface of the periderm (Pereira 2007) and their borders are composed by thicker cell walls (Pereira 2015), which show higher density. The porosity is affected by genetic and external factors as organisms or striping procedures and could be filled with a movable cellular material. Additionally, it can be

\*Corresponding author. Ana Patrícia Poeiras, e-mail: [apcp@uevora.pt](mailto:apcp@uevora.pt)

affected by management factors, as well, as the distance between trees (Marrafa 2016; Silva et al. 2017). Density affects positively or negatively the mechanical behaviour of cork, is responsible for the material flexibility and is related with the cork cells structure and the thickness of cork cells walls (Anjos et al. 2008).

The use of X-ray microdensitometer is commonly employed in wood science to analyse wood cores. It is the reference method in dendrochronology, used to measure growth rings, earlywood and latewood densities and wood density profiles (Jacquin et al. 2017; Dias et al. 2018). However, already in the mid-nineties, Fonseca et al. (1994) has explored the use of microdensitometry to determining cork quality: namely in the study of the density variation on the suberised tissues around the pores.

In the last decade, Oliveira et al. (2013, 2015, 2016) analysed the intern structure of cork stoppers by X-ray micro-computed tomography ( $\mu$ CT) and authors as Brunetti et al. (2002), Lagorce-Tachon et al. (2015) and Le Barbenchon et al. (2019) studied, using the same technique, the intern structure of cork and granulated cork stoppers. Moreover, as part of a study of imaging of cork over four hundred years, Crouvisier-Urien et al. (2019) also used the X-ray technology to assess the inner porosity in cork stoppers. This method allows the reconstruction of cross-sections of a cork sample into a 3D object based in a computer algorithm and shows internal defects by a non-destructive method. The  $\mu$ CT method was strongly described by authors as Stock (2009) and Rajczakowska et al. (2015) and in cork stoppers industry has proven to be an added value. Thus, for the reason that it helped and completed the manual chosen procedure. The  $\mu$ CT has been extensively used in wood science in areas such as: anatomical research, rings analysis and wood physical mechanical behaviour as shrinkage (Bulcke et al. 2009; Belini et al. 2011; Taylor et al. 2013; Van den Bulcke et al. 2014). The cork oak forest ecosystem is responsible for a healthier and profitable environment, employment in rural regions and is responsible for the economic growth that relies on cork production both in quantity and quality being the market price of cork a major economic drive of system management (Pinheiro et al. 2008; Ribeiro et al. 2010). However, climate changes are affecting all the species, including cork oak, as mentioned in numerous global and specific literature (Gouveia et al. 2017; Lionello et al. 2017; Seidl et al. 2017; Morin et al. 2018;). Due to natural irregularity of the climatic growth factors of precipitation and temperature, cork shows differences in its characteristics along harvests. Events of drought or intensive rainfall have relevant impact in the cork growth as it was described in several studies demonstrating the influence of annual precipitation on cork rings growth (Caritat et al. 1996; Costa et al. 2002; Leite et al. 2019). Cork characteristics such as growth and density are equally dependent on the implemented silviculture model and specific conditions (Ribeiro et al. 2021) and may be controlled by stand density and structure regulation over

time being possible to enhance final cork quality through management (Ribeiro et al. 2011; 2012). Modifications on the management systems in the last decades, mainly by mechanization (soil tillage) and/or intensification of agro-pastoral components are responsible for forest decline and jeopardize the cork quality production (Ribeiro et al. 2004, 2006, 2010; Camilo-Alves et al. 2013, 2017; Godinho et al. 2016; Pinto-Correia et al. 2018). Once the cork production could be at risk, with the reduction of raw material (Camilo-Alves et al. 2020) the application of irrigation systems in some places with available water, and with an efficient use of water, could contribute to increase the cork production.

The aim of this work was to study the principal features responsible for cork quality of those raw natural samples from specific regions in Portugal with two X-ray technologies ( $\mu$ CT and X-ray microdensitometry) trying to understand if both techniques can complement each other in this analysis. The  $\mu$ CT was used for the analysis of the intern porosity, enabling the cross-sections reconstruction along the sample (pith to bark), to understand how the porosity was developed along the cork growth direction and how it fluctuates over time (over harvests). Density and radial growth were analysed with X-ray microdensitometry technology, as in Poeriras et al. (2021) about the cork characteristics from a specific water regime. These two techniques were approached and their potentialities and limitations were evaluated in this study, allowing to understand better the cork features.

## 2. Material and methods

### 2.1. Sampling and study sites

Raw cork samples from two different sites, all from reproduction cork at 130 cm height, were analysed. The research sites are maintained by the University of Évora and have a different silviculture treatment. Treatments are named Site 1 and Site 2 in the consecutive text.

Site 1: eighteen cork samples from three consecutive harvests (1999, 2008 and 2017) at the same trees (6 trees  $\times$  3 years of harvest). Samples had 8 complete years of growth, harvested in 9 and 9 years, and the site was under its natural environmental conditions, rainfed only (Table 1). Precipitation decreased from the first harvest until the third one. Soil varying between Cambisols and Arenosols: Cambisols presented sandy loam of finer subsurface horizons with fast permeability, which come from the mother rock intensively changed. They are commonly used for agriculture and forestry (PROF, ICNF 2019). On the other hand, Arenosols are sandy-textured with any significant soil profile development, with excessive permeability.

Site 2: six cork samples harvested in 2017 with 5 complete years of growth, with the same age that 2017' harvest in the Site 1. Although the natural environmental conditions, related with the average annual precipita-

tion (Table 1), the site was subjected to a different water regime: Irrigation occurred once a week, from June to October, averaging  $1928 \text{ m}^3 \text{ ha}^{-1}$  per year (Poeiras et al. 2021). Soil was a Gleyic luvisol low saturated, which presented hydromorphic properties within 50 cm of the surface (FAO 2020).

**Table 1.** Annual precipitation at the study sites, distributed by periods of annual rings cork growth.

Average annual precipitation [ $\text{mm year}^{-1}$ ]				
Period of cork growth	1991–1999	2000–2008	2009–2017	2012–2017
Site 1	589.88	530.56	408.22	
Site 2				528

We decided to study of the volume fraction of lenticels along harvests in the Site 1 and between the last harvest of the Site 1 and Site 2, using micro-computed tomography (SkyScan, Bruker, Belgium), and the density and growth at the same samples, with QTRS-01X Tree Ring Analyser (Quintek Measurement Systems Inc., Knoxville, TN, USA) (Fig. 1). The same technique of X-ray microdensitometry to study growth and density was used in Poeiras et al. 2021, but now we intend also to understand if both techniques can complement each other.

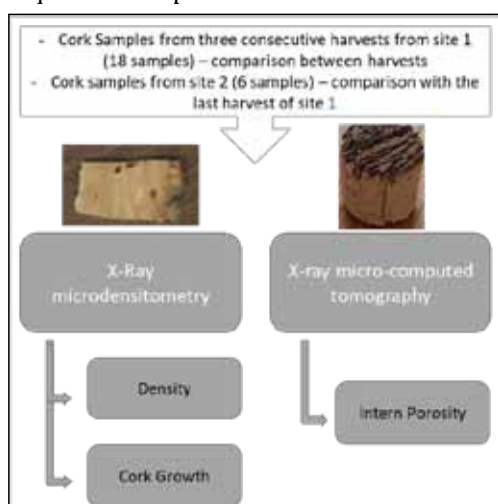


**Fig. 1.** General scheme about samples, used X-ray techniques and measured parameters measured in each one of the techniques.

In the sub-chapters related with the comparison between the 3<sup>rd</sup> harvest of the Site 1 and Site 2 (both in

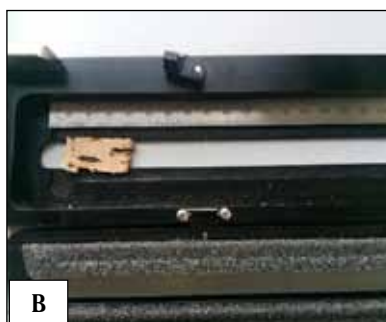


**Fig. 2.** A – QTRS-01X Data Analyser and Scanner (Quintek Measurement Systems Inc., Knoxville, TN, USA); B – Cassette where the sample is positioned.

2017), is called the Treatment 0 and Treatment 1, respectively, due to the water regime applied in the Site 2.

## 2.2. X-ray microdensitometry analysis

Density and growth analysis were obtained by QTRS-01X Tree Ring Analyser (Quintek Measurement Systems Inc., Knoxville, TN, USA) on radial slices with 1.5 cm thickness (Fig. 2), cut with a slicer machine (ABO with 220 mm incorporate blade and sharpener, Oggiona VA, Italy). One measurement per sample were performed (24 in total). The first and last rings (half rings) corresponding to pith and to bark of cork samples were not considered for the analysis. Measurements were achieved automatically with QTRS-01X software, which were based on the principle of absorption of radiation from a collimated beam of X-rays. The density calculation at each measurement point was done from the ratio of the measured attenuation and the beam intensity. The mass attenuation coefficient depends on the energy of the incident radiation and the material composition, which water is the integral element in the measurement accuracy. The microdensitometry analysis provides the capability to recognize the differences in autumn and spring rings cork density and rings growth.

Calibration were done with a mass absorption coefficient of 3.80, a threshold of 200 and a dead band of 50. The radiation beam passed through the sample (bark to pith direction), which length was changed according to each sample. The target density on the calibration parameters was defined as  $0.250 \text{ g cm}^{-2}$ , as the maximum in cork density, according Fortes et al. (2004) and Anjos et al. (2008).

## 2.3. X-ray micro-computed tomography ( $\mu\text{CT}$ ) analysis

Samples (18 + 6) were turned into cylinders with a diameter of 25 mm (one cylinder per sample) (see Fig. 3A). A turnstile press machine, from pith to bark, was used in order to fit the tube base of the  $\mu\text{CT}$  equipment (SkyScan, Bruker, Belgium). Samples were maintained at regular environmental conditions.

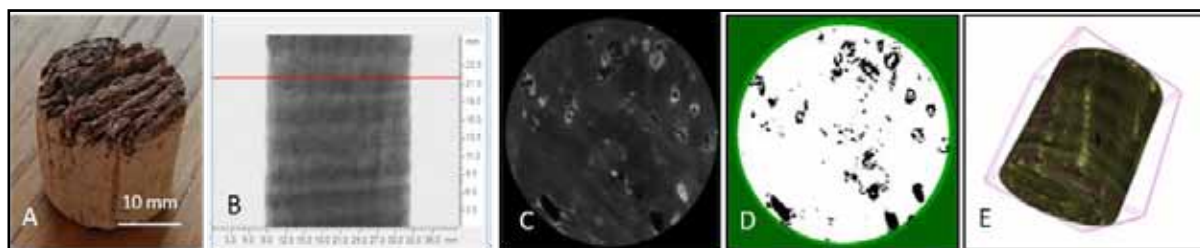


**Fig. 3.** Sequence of image processing: A – cylindrical cork sample prepared for microCT analysis; B – 1st projection image of a cork sample acquired with CTAn version 1.14.4.1+ (64-bit), Bruker microCT; C – reconstructed cross-section of the cork sample (raw image); D – reconstructed cross-section of the cork sample under binarization; E – 3D reconstruction with CTVOx (CTVOx version 3.0.0r1114 (64-bit)).

The general principles and applications of X-ray micro computed tomography have been described in some literature (Elliott et al. 1990; Rajczakowska et al. 2015) – an attenuated X-ray beam passes through the sample and a reconstruction of the sample, through a set of cross-sections, is performed automatically using mathematic algorithms. It is a non-destructive method, without cell damage during the process of sample's preparation.

The X-ray tube was tuned down to 50 Kv and 800  $\mu$ A and the projection images were captured with an exposure time of 2200 ms over a 180° rotation with a 31  $\mu$ m pixel size. The process resulting in a total acquisition time of 1 h per sample. NRecon (SkyScan1174v2, Bruker microCT, Belgium, version 1.1) was used to make the reconstruction images via the filtered back projection algorithm. The parameters used in the reconstruction of all the databases were: smoothing – 8; ring artefact correction – 13; sharpening – 40%; beam hardening correction – 28%.

Data Analyser (CTAn SkyScan, Bruker micro CT, Belgium, version 1.14.4.1) was used to analyse the intern structure and the volume fraction of lenticels. After the image acquisition, a Volume of Interest (VOI) was chosen for each sample and images were binarized for the analysis (Fig. 3B and 3C). In the binarization the lenticular channels (empty spaces) appeared in black and the solid

material in white (Fig. 3D), which histogram was 24–74 for every sample. The lenticular channels present different shapes when visualized from radial and tangential sections, as lengthened and circular shapes, respectively, observed in DataViewer (Version 1.5.1.2 64-bit, SkyScan, Bruker microCT) (Fig. 4A and 4B).

Then, total, close and open porosity were automatically calculated for each sample, in 3D analysis. The porosity along samples was measured in specific cross sections (corresponding to 6 to 18 mm for each volume of interest), in 2D automatically analysis. The pores' area was manually measured and the pores counted, from the binarized images, at the same cross sections. The CTVOx (SkyScan, Bruker micro CT, Belgium, 3.0.0r1114, 64-bit) was used to do the realistic 3D visualization related with the X-ray absorption in the different slices of the object (Fig. 3E and Fig. 5).

## 2.4. Statistical analysis

Statistical analysis was made using SPSS v.25 software package (IBM Corp., Armonk, NY, USA). Analysis of Variance (ANOVA) was done to compare samples from different years of harvest and different treatments. General Linear Models (GLM) of Gauss normal distribution of fitted model were applied to compare the main effects

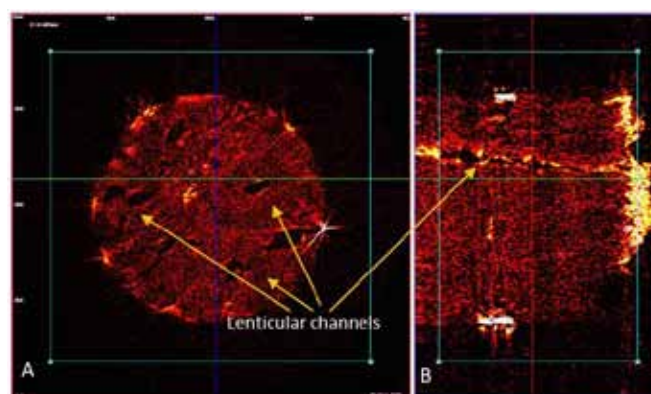


**Fig 4.** Tangential section (A) and radial section (B) from a cork sample, obtained with DataViewer (Version 1.5.1.2 64-bit, SkyScan, Bruker microCT): A) shows lenticular channels with circular shapes (in yellow) and B shows one elongated lenticular channel (in yellow).



**Fig 5.** 3 – D reconstruction using CTvox version 3.0.0r1114 (64-bit). Image on the left represents a complete sample and image on the right represents a volume of interest (VOI).

and evaluate the significant differences between the group of means from each harvest and treatment.

In the consecutive text,  $p > 0.05$  is used as not significant;  $p < 0.05$  is used as significant;  $p < 0.01$  is used as very significant and  $p < 0.001$  as highly significant, in terms of the statistical explanation.

### 3. Results

#### 3.1. Cork density and growth analysis with X–ray microdensitometry technology

##### 3.1.1 Harvests in the Site 1

The X–ray microdensitometry technology was used to analyse the total density and growth per sample and per individual cork ring. Samples revealed an increasing on average total density over extractions (from 1999 to 2017) and a decreasing on total growth. The same happened on the density and growth checked on the cork rings (Table 2).

**Table 2.** Means  $\pm$  Std. deviation of total density, average ring density, cork thickness and average cork-ring width according the year of harvest, from the Site 1.

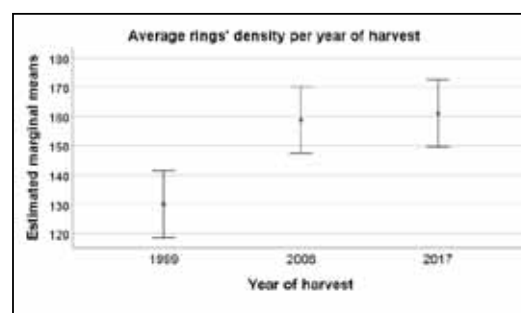
Year of harvest	Total density	Ring density	Cork thickness	Cork-ring width
	[g cm <sup>-3</sup> ]			
1999	0.130 $\pm$ 0.019	0.130 $\pm$ 0.030	28.22 $\pm$ 7.64	3.52 $\pm$ 1.48
2008	0.153 $\pm$ 0.028	0.159 $\pm$ 0.056	26.47 $\pm$ 4.22	3.30 $\pm$ 1.32
2017	0.157 $\pm$ 0.020	0.161 $\pm$ 0.036	23.61 $\pm$ 6.85	2.94 $\pm$ 1.43

Table 3 shows the results from the analysis of variance for the year of harvest on the different cork-ring thickness regarding density and ring-width.

**Table 3.** Analysis of variance for the year of harvest on the different rings of cork growth, regarding density (in g per cm<sup>3</sup>) and cork-ring width (in mm).

Source of variation	DF	Density		Ring width	
		F	P value	F	P value
Year of harvest	2	9.055	<0.0001	2.284	0.106
Ring	7	3.004	0.006	4.166	<0.0001
Year of harvest * Ring	14	1.199	0.285	0.602	0.859
Residual	120	—	—	—	—

The year of harvest represented a highly significant influence ( $p < 0.0001$ ) in cork density. Nevertheless, only the year of 1999 showed a different statistical density (Fig. 6). However, it did not show significance due to cork growth ( $p = 0.106$ ) (Fig. 7). The rings of cork formation (Fig. 8 and Fig. 9) showed very significant variation in regard to density and highly significance regarding ring width. The interaction between each year of harvest and ring did not represent a significant effect on density and ring-width ( $p = 0.285$  and  $p = 0.859$ , respectively; Table 3).



**Fig 6.** Result of density (in g cm<sup>-3</sup>) analysis in three consecutive harvests (average per cork ring). Error bars indicate 95% CI.

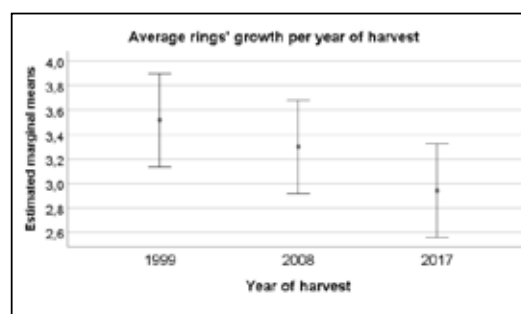


**Fig 7.** Result of the average cork-ring width (in mm) analysis in three consecutive harvests. Error bars indicate 95% CI.

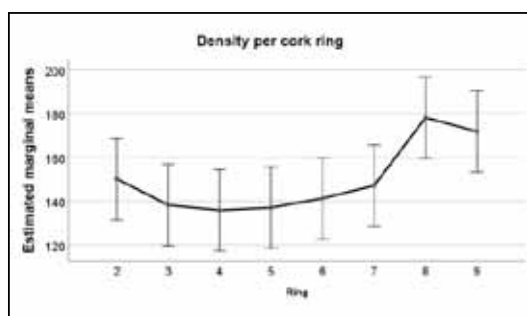


**Fig 8.** Result of density (in  $\text{g cm}^{-3}$ ) analysis over cork thickness. Error bars indicate 95% CI.

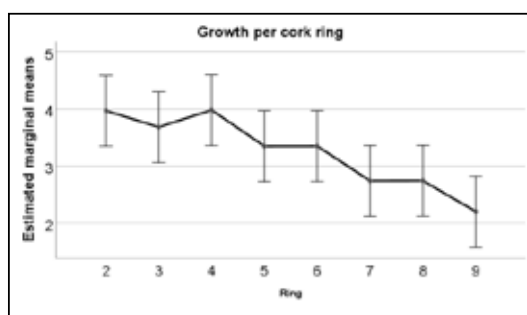


**Fig 9.** Result of cork-ring width (in mm) analysis over cork thickness. Error bars indicate 95% CI.

### 3.1.2 Comparison between the 3<sup>rd</sup> harvest of the Site 1 and Site 2

When compared the 3<sup>rd</sup> harvest of the Site 1 (non-irrigated) and Site 2 (subjected to irrigation), the results demonstrated higher total growth and higher growth per ring in cork from the Site 2. On the other hand, the density was lower in the total sample and per ring (Table 4). The comparisons per ring were performed on the same five years of growth in both treatments.

**Table 4.** Mean  $\pm$  Std. deviation of total density, ring density, cork thickness and cork-ring width according to the treatment (0 – non-irrigated; 1 – irrigated).

Treatment	Total density	Ring density	Cork thickness	Cork-ring width
	[ $\text{g cm}^{-3}$ ]		[mm]	
0	$0.157 \pm 0.020$	$0.154 \pm 0.026$	$23.61 \pm 6.85$	$3.23 \pm 1.62$
1	$0.144 \pm 0.021$	$0.148 \pm 0.041$	$25.50 \pm 1.86$	$5.09 \pm 1.36$

The results obtained from ANOVA (Table 5) demonstrated a highly significant influence of the different water regime (Treatment) in the cork growth ( $p < 0.0001$ ) (Fig. 10) Even with the differences of the means related with density, ANOVA did not show significance ( $p = 0.475$ ) (Fig. 11). Rings demonstrated to be a significant origin of variation for density but did not show significance for cork-ring width. The interaction between treatment and rings showed significance for density and ring width (0.049 and 0.022, respectively).

**Table 5.** Analysis of variance for treatment on the different samples and rings, regarding density (in  $\text{g cm}^{-3}$ ) and cork-ring width (in mm).

Source of variation	DF	Density		Ring width	
		F	P value	F	P value
Treatment	1	0.518	0.475	28.116	<0.0001
Ring	4	3.223	0.020	1.915	0.123
Treatment * Ring	4	2.577	0.049	3.141	0.022
Residual	50	—	—	—	—

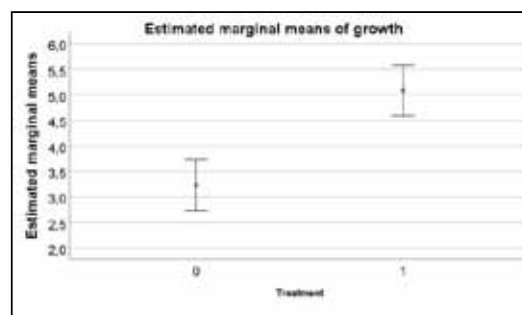


**Fig. 10.** Result of growth analysis in treatments 0 and 1 (average per ring of cork growth). Error bars indicate 95% CI.

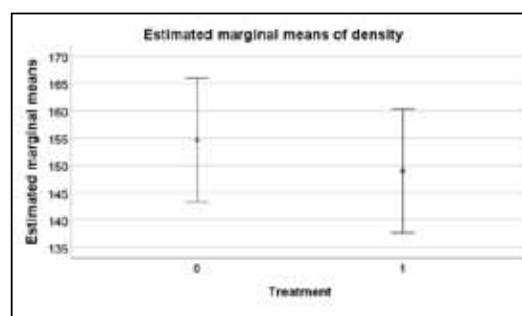


**Fig. 11.** Result of density analysis in treatments 0 and 1 (average per ring of cork growth). Error bars indicate 95% CI.

## 3.2. Intern porosity with X-ray $\mu$ CT technology

### 3.2.1 Harvests in the Site 1

Total, open and close porosity, in 3D analysis, were automatically measured in CT Analyser (SkyScan, Bruker micro CT, Belgium, version 1.14.4.1) for each group of samples (harvests of 1999, 2008 and 2017). The analysis demonstrated an increasing of total and open porosity over years, and a slight regression of close porosity from the first harvest to the second one (Table 6).

**Table 6.** Mean  $\pm$  Standard deviation of total, open and close porosity regarding the harvests.

Year	Total porosity	Open porosity	Close porosity
	[%]		
1999	$17.02 \pm 6.70$	$14.96 \pm 7.01$	$2.41 \pm 0.73$
2008	$17.58 \pm 7.15$	$15.90 \pm 7.27$	$2.00 \pm 0.48$
2017	$18.47 \pm 6.89$	$16.34 \pm 7.04$	$2.54 \pm 1.02$

The results obtained from the ANOVA (Table 7) did not verify a significant influence of the year of harvest in total porosity. Only the source of variation samples within each year of harvest showed a highly significance. These analyses demonstrated high variability in the different samples. A high variability within each cross section was markedly presented and the interaction cross-section and year of harvest did not exist.

**Table 7.** Analysis of variance for the year of harvest on the different samples and cross-sections, regarding the total porosity (in per cent).

Source of variation	Total porosity		
	DF	F	P value
Year of harvest	2	0.789	0.456
Sample/Year of harvest	15	5.823	<0.0001
Cross-section	12	0.953	0.496
Cross-section x Year of harvest	24	0.950	0.534
Residual	180	—	—

The findings from the analysis of variance are shown in the Fig. 12 and Fig. 13.

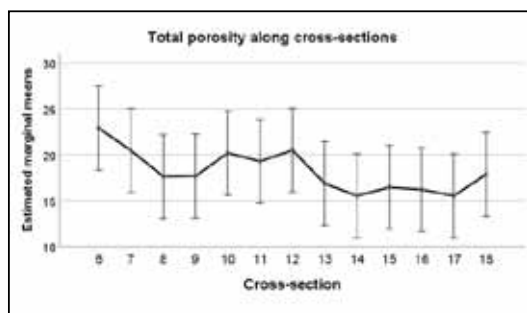


**Fig. 12.** Total porosity (in per cent) along cross-sections (6–18 mm). Error bars indicate 95% CI.

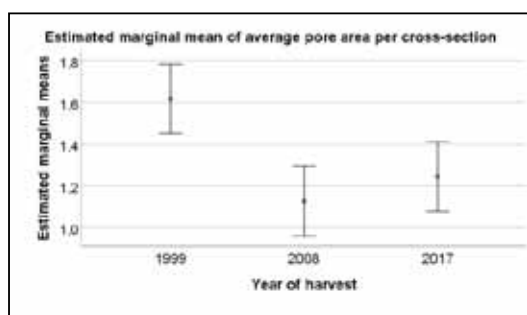


**Fig. 13.** Result of total porosity (in per cent) per cross-section on each year of harvest. Error bars indicate 95% CI.

At the same time, the evolution of total porosity along cork samples (from pith to bark) in 2D cross-sections between 6 and 18 mm were automatically analysed for each sample. For this intention one millimeter correspond to one cross-section. Higher pores' area was measured in the first harvest. However, the higher number of pores belong to the last harvest.

The ANOVA with regard to the number of pores (Table 8) showed a highly significance for all of the sources of variation. The interaction between cross-

section and the year of harvest was the only source of variation that demonstrated to be not significant (Fig. 14 and Fig. 15).

**Table 8.** Analysis of variance for the year of harvest on the different samples and cross-section, regarding the number of pores and pores' area.

Source of variation	Number of pores			Pores' area [mm <sup>2</sup> ]	
	DF	F	P value	F	P value
Year of harvest	2	7.718	<0.0001	12.586	<0.0001
Sample/Year of harvest	15	35.481	<0.0001	10.146	<0.0001
Cross-section	12	6.186	<0.0001	1.835	<0.038
Cross-section x Year of harvest	24	4.074	<0.0001	0.595	0.940
Sample x (cross-section/Year of harvest)	180	2.306	<0.0001	1.462	<0.0001
Residual	4560	—	—	—	—

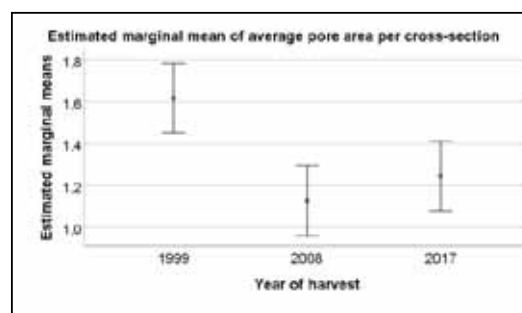


**Fig. 14.** Result of pores' area (in mm<sup>2</sup>) per cross-section on each year of harvest. Error bars indicate 95% CI.

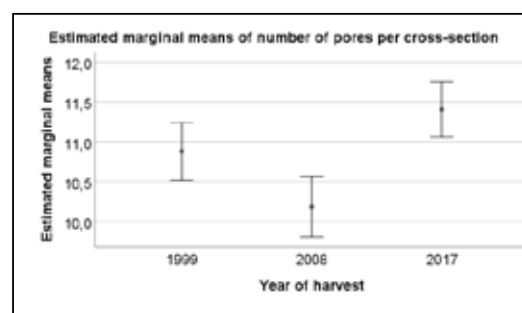


**Fig. 15.** Result of number of pores per cross-section on each year of harvest. Error bars indicate 95% CI.

### 3.2.2 Comparison between the 3<sup>rd</sup> harvest of the Site 1 and Site 2

Total, open and close porosity, in a 3D analysis in CT Analyser, regarding the complete sample, demonstrated to be higher in the Treatment 1, subjected to a different water regime, when contrasted with the Treatment 0 (the last harvest of the Site 1) (Table 9).

**Table 9.** Mean ± Std. deviation of total, open and close porosity according to the treatment.

Treatment	Total porosity	Open porosity	Close porosity
		[%]	
0	18.47 ± 6.89	16.34 ± 7.04	2.54 ± 1.02
1	27.87 ± 9.98	25.77 ± 10.41	2.80 ± 0.96

Along cross-sections, between 6 and 18 mm, the 2D analysis also revealed an evident difference between treatments, with higher values in the Treatment 1 (Fig. 16).

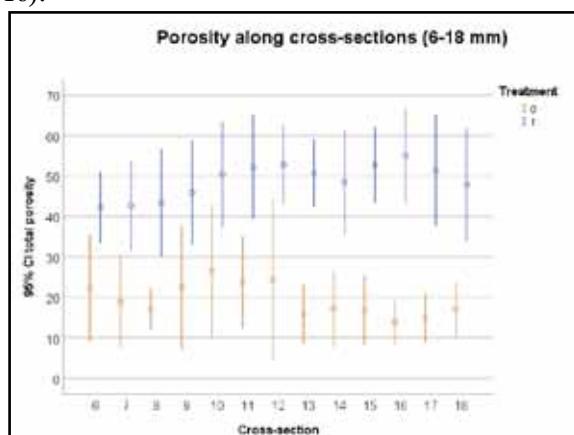


Fig. 16. Total porosity along cross-sections in the treatments 0 and 1.

The pores' area was bigger in samples from the Treatment 1 (Fig. 17) while the number of pores counted was smaller.

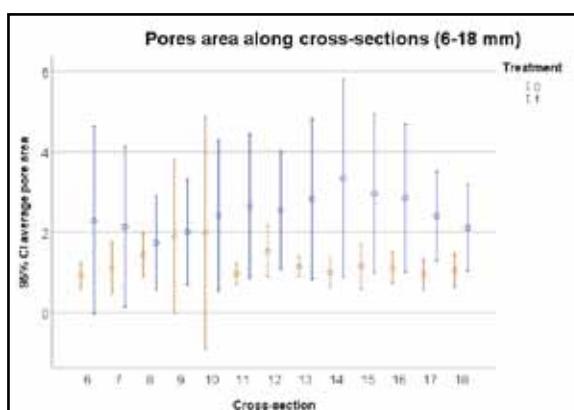


Fig. 17. Pores' area per mm<sup>2</sup> regarding the treatment, along cross-sections (6–18 mm).

The statistical analysis (ANOVA) revealed a highly significant influence of treatment and samples within each treatment for total porosity and pores' area ( $p < 0.0001$ ) (Tables 10 and 11). The irrigation demonstrated a significant impact on the porosity and pores' area analysed, but was not statistically significant in regard the number of pores. Cross-sections did not demonstrate significance on the total porosity and in the pores area, but revealed a highly significance in the number of pores.

Table 10. Analysis of variance for the total porosity (in per cent) according to the treatment, samples and cross-section.

Source of variation	DF	Total porosity	
		F	P value
Treatment	1	493.922	<0.0001
Sample/Treatment	10	10.331	<0.0001
Cross-section	12	1.302	0.226
Cross-section x Treatment	12	1.674	0.081
Residual	120	—	—

Table 11. Analysis of variance for treatment on the different samples and cross-section, regarding the number of pores and pores' area.

Source of variation	DF	Number of pores		Pores' area [mm <sup>2</sup> ]	
		F	P value	F	P value
Treatment	1	1.722	0.190	94.851	<0.0001
Sample/Treatment	10	24.935	0.0001	13.852	<0.0001
Cross-section	12	6.827	0.0001	1.221	0.261
Cross-section x Treatment	12	4.201	0.0001	1.851	0.036
Sample x (Cross-section/Treatment)	120	2.526	0.0001	1.494	0.001
Residual	3213	—	—	—	—

Figures 18, 19 and 20 confirmed the results from the analysis of variance.

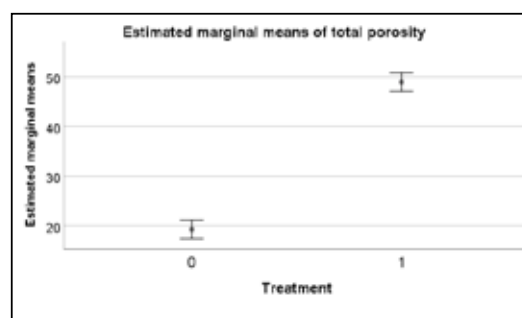


Fig. 18. Result of total porosity (in %) per cross-section on each treatment. Error bars indicate 95% CI.

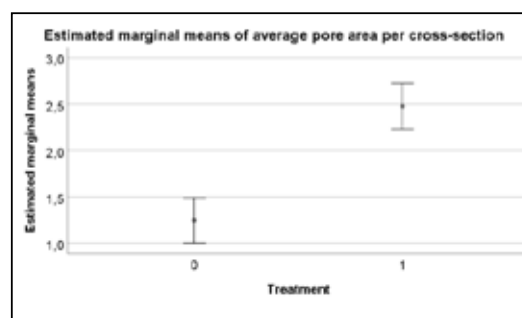


Fig. 19. Result of pores' area (in mm<sup>2</sup>) on each treatment. Error bars indicate 95% CI.

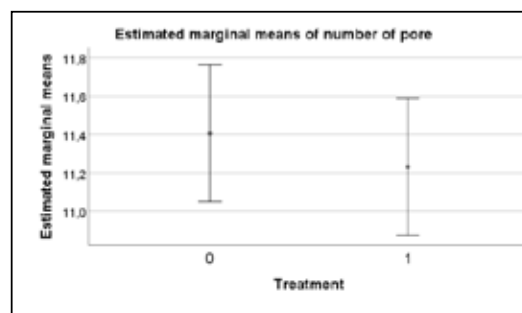


Fig. 20. Result of number of pores on each treatment (measured per cross-section). Error bars indicate 95% CI.

#### 4. Discussion

A reduction on cork growth over harvests for the same trees was found with the X-ray microdensitometer, at the same time that an increasing on cork density was



revealed. The reduction of growth can be explained by the changes on precipitation – the drops over time cause reductions on cork growth, which is according to literature (Costa et al. 2016; Leite et al. 2019).

For each cork sample, the growth curve (Fig. 9) showed a decreasing cork growth trend, explained by Natividade (1934), Fortes et al. (2004) and Ghalem et al. (2016) which is related with the pressure caused by the oldest rings and external enclosure. However, the density curve (Fig. 8) showed an increasing on cork density trend, which can be explained by the smaller growths in the newest rings and consequent lower number of spring cells with thinner cell walls (Natividade 1934). Once the density analysis was performed in raw cork, the densification of the external rings may be due to the cellular tensions occurred in the radial cork growth.

When compared cork samples from the two different site managements, cork from the Treatment 1 (irrigated) showed higher growth rates. According literature drought episodes are the responsible for low cork growth (Costa et al. 2016) so the higher growth rates can be explained by the conditions that trees have – more water availability. The higher growth of cork from the plot subjected to irrigation contributes to the increasing on cork production.

Despite the lower density presented in cork from the irrigated plot, the statistical analysis did not reveal any significance related with the management, in contrast to cork growth. As Natividade (1934) demonstrated, higher growths showed bigger cells, which correspond to bigger spring cells. Because of that, density is related with cork growth and not directly with the site management. Fonseca et al. (1994) found a negative correlation between the average width of growth and the cork density, which was statistically significant, but only 8.6%.

The findings related with the values of density for samples from both plots ( $0.157 \pm 0.020$  g per  $\text{cm}^3$  in the Site 1 – non-irrigated – and  $0.144 \pm 0.021$  g per  $\text{cm}^3$  in the Site 2 – irrigated) were in line with bibliography and suitable for the industry. Knapić et al. (2016) and Pereira (2007) mentioned valued of 0.120–0.170 g per  $\text{cm}^3$ .

Regarding the  $\mu\text{CT}$  analysis, the  $\mu\text{CT}$  images resolution depends on the scanner used, which was lower in the Bruker Skyscanner used for this study. Moreover, cork tissue has a lower density compared with other materials, as bone, concrete or wood, largely analysed with  $\mu\text{CT}$  technology. As a result of that, some issues related with the cross-sections threshold occurred in the visualization of the lenticular channels in 3D and 2D analysis. However, it was possible to perform the purpose of this analysis. In the 3D analysis, used for the general porosity acquisition, the porosity is smaller than in the 2D analysis (used for a specific volume of interest along cork samples – porosity on cross-sections). These happened due to the close porosity (pores are more probably surrounded by solid material in the 2D sections).

Open porosity was higher than close porosity in every year of harvest and plots, which is related with the inner structure of cork. Lenticular channels cross the cork plank radially, from the phellogen to the external surface, allowing gas exchanges (Oliveira & Pereira 2020).

The year of harvest and samples in each year showed to be relevant sources of variation in regard to pores area and number of pores. In every analysis samples in each year demonstrated to be a highly significant origin of variation, which shows the genetic variability presented in cork and the importance of the genetic factors in those characteristics (identical findings were presented by Silva (1996)).

Our results suggested that the formation of lenticels could not only be controlled by genetic factors, as referred by Pereira (2007). The increasing on density over harvests for the same plot (which accompanying the increase of porosity on the same samples) could be related by the thicker cell walls – sclereid cell walls – surrounding the lenticular channels (Fonseca et al. 1994; Pereira 2015). Total porosity and the pores area were not influenced by the cross-sections, as showed by the statistical analysis. However, the number of pores was influenced by the position in samples, which suggest their emergence or disappearance along the cork profile or can be related with the discontinuities presented in cork (Fortes et al. 2004).

When samples from the different management plots were compared the results demonstrated a notorious difference on them. The treatment highly influenced the porosity, pores area and number of pores, which demonstrated that the management practices revealed an impact on porosity. The Treatment 1 (irrigated) brought an increasing on porosity due to pores' area and not due to the number of pores. According Natividade (1934) the favourable growth conditions presented in a plot originate a faster cork growth, which contributes to the deformation of lenticular channels. The bigger pores area found in the Treatment 1 could be explained by that. Variability is markedly present on both sites, represented by the source of variation samples within each treatment, which shows that the genetic factors continuous to be one of the most important factors in the variability of cork quality (Pereira 2007; Silva et al. 2017).

## 5. Conclusions

The comparison of cork porosity between consecutive harvests and between the 3<sup>rd</sup> harvest of the Site 1 and Site 2 were quantified in those intern structure with  $\mu\text{CT}$  technology, and characteristics as density and total growth were measured with microdensitometry technology.

Both techniques demonstrated to be valuable for the present analysis. The use of  $\mu\text{CT}$  could be an opportunity in further studies to compare the inner porosity of cork from *Quercus suber* L. with the surface coefficient porosity of the same samples, in different site managements.

$\mu$ CT proved to be an important technique to analyse open and close porosity, quantify pores and measure pores' area along cork samples. At the same time, the X-ray microdensitometry was confirmed as a relevant technique that may be used in the same samples as  $\mu$ CT (after sectioning in slices), to study the density and growth of cork profiles, in a 2D analysis. Regarding density and growth, the microdensitometry has the advantage of measure distinctly each cork ring, which was not correctly visualized in  $\mu$ CT analysis. However, to use the microdensitometer is required to convert samples in thinner slices, which is more time-consuming. The techniques used can complement each other and contribute to the main cork features analysis.

Our experiment clearly demonstrated that irrigation can increase cork production, thus it is possible to control the cork growth through the silviculture model. Additionally, management practices shown to have a contribution to changes in cork features. In future studies the number of samples could be duplicated with the goal of cover a larger number of trees from different sites with a variety of silviculture models.

## Acknowledgements

This research was funded by “Medida 4.1–Cooperação para a Inovação/ProDeR 52131 and 52132”, by PDR2020-101-FEADER-031427 “GO-RegaCork”; by a master grant from Prodehesa Montado Project – Reference 0276\_PRODEHESA\_MONTADO\_6, by the Strategic Project (UIDB/04033/2020) of CITAB, by national funding from Fundação para a Ciência e a Tecnologia (FCT) and by Czech University of Live Sciences Prague for the research developed in FLD laboratory.

## References

- Anjos, O., Pereira, H., Rosa, M., 2008: Effect of quality, porosity and density on the compression properties of cork. *Holz Als Roh – Und Werkstoff*, 66:295–301.
- Barbenchon, L., Girardot, J., Kopp, J., Viot, P., 2019: Multi-scale foam : 3D structure/compressive behaviour relationship of agglomerated cork. *Materialia*, 5:100219.
- Belini, U., Tomazello, M., Castro, V., Muniz, G., Lasso, P., Vaz, C., 2011: Microtomografia de Raios X (microCT) Aplicada na Caracterização Anatômica da Madeira de Folhosa e de Conifera. *Floresta e Ambiente*, 18:30–36.
- Brunetti, A., Cesareo, R., Golosio, B., Luciano, P., Ruggero, A., 2002: Cork quality estimation by using Compton tomography. *Nuclear Instruments and Methods in Physics Research, Section B: Beam Interactions with Materials and Atoms*, 196:161–168.
- Bulcke, J., Boone, M., Acker, J., Stevens, M., Hoorebeke, L., 2009: X-ray tomography as a tool for detailed anatomical analysis. *Annals of Forest Science*, 66:508–508.
- Bulcke, J., Wernersson, E., Dierick, M., Loo, D., Masschaele, B., Brabant, L. et al., 2014: 3D tree-ring analysis using helical X-ray tomography. *Dendrochronologia*, 32:39–46.
- Camilo-Alves, C., Clara, M., Ribeiro, N., 2013: Decline of Mediterranean oak trees and its association with *Phytophthora cinnamomi*: A review. *European Journal of Forest Research*, 132:411–432.
- Camilo-Alves, C., Dinis, C., Vaz, M., Barroso, J., Ribeiro, N., 2020: Irrigation of young cork oaks under field conditions-testing the bestwater volume. *Forests*, 11:1–15.
- Camilo-Alves, C., Vaz, M., Clara, M., Ribeiro, N., 2017: Chronic cork oak decline and water status: new insights. *New Forests*, 48:753–772.
- Caritat, A., Molinas, M., Gutierrez, E., 1996: Annual cork-ring width variability of *Quercus suber* L. in relation to temperature and precipitation (Extremadura, southwestern Spain). *Forest Ecology and Management*, 86:113–120.
- Costa, A., Pereira, H., Oliveira, A., 2002: Influence of climate on the seasonality of radial growth of cork oak during a cork production cycle. *Annals of Forest Science*, 59:429–437.
- Costa, A., Barbosa, I., Roussado, C., Graça, J., Spiecker, H., 2016: Climate response of cork growth in the Mediterranean oak (*Quercus suber* L.) woodlands of southwestern Portugal. *Dendrochronologia*, 38:72–81.
- Crouvisier-Urien, K., Chanut, J., Lagorce, A., Winckler, P., Wang, Z., Verboven, P. et al., 2019: Four hundred years of cork imaging: New advances in the characterization of the cork structure. *Scientific Reports*, 9:19682.
- Dias, A., Gaspar, M., Carvalho, A., Pires, J., Lima-Brito, J., Silva M. et al., 2018: Within - and between - tree variation of wood density components in *Pinus nigra* at six sites in Portugal. *Annals of Forest Science*, 75:58.
- Elliott, J., Anderson, P., Davis, G., Dover, S., Stock, S., Breunig, T. et al., 1990: Application of X-ray microtomography in materials science illustrated by a study of a continuous fiber metal matrix composite. *Journal of X-ray Science and Technology*, 2:249–258.
- Fonseca, F., Louzada, J., Silva, M. 1994: Crescimento e Qualidade da Cortiça: Potencialidades da Microdensitometria. III Congresso Florestal Nacional- “Os recursos florestais no desenvolvimento rural”. Sociedade Portuguesa de Ciências Florestais. Figueira da Foz. *Actas*, 2:267–279.
- Fortes, M., Rosa M., Pereira H., 2004: A Cortiça. IST Press, 260 p.
- Ghalem, A., Barbosa, I., Bouhraoua, R., Costa, A., Delloio, R., 2016: Comparing cork quality from Hafir-Zariffet mountain forest (Tlemcen, Algeria) vs. Tagus basin Montado (Benavente, Portugal). *Cogent Biology*, 2:1236431.

- Godinho, S., Guiomar, N., Machado, R., Santos, P., Sá-Sousa, P., Fernandes, J. et al., 2016: Assessment of environment, land management, and spatial variables on recent changes in montado land cover in southern Portugal. *Agroforestry Systems*, 90:177–192.
- Gouveia, C., Trigo, R., Beguería, S., Vicente-Serrano, S., 2017: Drought impacts on vegetation activity in the Mediterranean region: An assessment using remote sensing data and multi-scale drought indicators. *Global and Planetary Change*, 151:15–27.
- Jacquín, P., Longuetaud, F., Leban, J., Mothe, F., 2017: X-ray microdensitometry of wood: A review of existing principles and devices. *Dendrochronologia*, 42:42–50.
- Knapic, S., Oliveira, V., Machado, J., Pereira, H., 2016: Cork as a building material: a review. *European Journal of Wood and Wood Products*, 74:775–791.
- Lagorce-Tachon, A., Karbowiak, T., Loupiac, C., Gaudry, A., Ott, F., Alba-Simionesco, C. et al., 2015: The cork viewed from the inside. *Journal of Food Engineering*, 149:214–221.
- Leite, C., Oliveira, V., Lauw, A., Pereira, H., 2019: Cork rings suggest how to manage *Quercus suber* to mitigate the effects of climate changes. *Agricultural and Forest Meteorology*, 266–267:12–19.
- Lionello, P., Özsoy, E., Planton, S., Zanchetta, G., 2017: Climate Variability and Change in the Mediterranean Region. *Global and Planetary Change*, 151:1–3.
- Marrafa, S., 2016: Evaluation of Cork Quality in 3 consecutive debarkings: Influence of tree and plot structure. Master Thesis Dissertation. University of Trás-os-Montes e Alto Douro, Vila Real, 60 p.
- Morin, X., Fahse, L., Jactel, H., Scherer-Lorenzen, M., García-Valdés, R., Bugmann, H., 2018: Long-term response of forest productivity to climate change is mostly driven by change in tree species composition. *Scientific Reports*, 8:1–12.
- Natividade, J. V., 1934: Cortiças – Contributo para o estudo do melhoramento da qualidade. Volume I. Direção Geral dos Serviços Florestais e Agrícolas, 143 p.
- Oliveira, V., Knapic, S., Lopes P., Cabral, M., Pereira, H., 2013: Incork. Avaliação da influência interna na transmissão de oxigénio de rolhas de cortiça natural por técnicas não destrutivas. 7º Congresso Florestal Nacional – Florestas: Conhecimento e Inovação, 349 p.
- Oliveira, V., Lopes, P., Cabral, M., Pereira, H., 2015: Influence of cork defects in the oxygen ingress through wine stoppers: Insights with X-ray tomography. *Journal of Food Engineering*, 165:66–73.
- Oliveira, V., Bulcke, J., Acker, J., Schryver, T., Pereira, H., 2016: Cork structural discontinuities studied with X-ray microtomography. *Holzforschung*, 70:87–94.
- Oliveira, V., Pereira, H., 2020: Cork and Cork Stoppers: Quality and Performance. *Winemaking – Stabilization, Aging Chemistry and Biochemistry*, p. 1–19.
- Pereira, H., 2007: The formation and growth of cork. *Cork*, p. 7–31.
- Pereira, H., 2015: The rationale behind cork properties: A review of structure and chemistry. *BioResources*, 10:6207–6229.
- Pinheiro, A., Ribeiro, N., Surový, P., Ferreira, A., 2008: Economic implications of different cork oak forest management systems. *International Journal of Sustainable Society*, 1:149–157.
- Pinto-Correia, T., Guiomar, N., Ferraz-de-Oliveira, M., Sales-Baptista, E., Rabaça, J., Godinho, C., et al., 2018: Progress in Identifying High Nature Value Montados: Impacts of Grazing on Hardwood Rangeland Biodiversity. *Rangeland Ecology and Management*, 71:612–625.
- Poeiras, A., Silva, M., Günther, B., Vogel, C., Surový, P., Ribeiro, N., 2021: Cork influenced by a specific water regime – macro and microstructure characterization: the first approach. *Wood Science and Technology*, 55:1653–1672.
- Rajczakowska, M., Stefaniuk, D., Łydzba, D., 2015: Microstructure Characterization by Means of X-ray Micro-CT and Nanoindentation Measurements. *Studia Geotechnica et Mechanica*, 37:75–84.
- Ribeiro, N., Dias, S., Surový, P., Gonçalves A., Ferreira, A. Oliveira A., 2004: The importance of crown cover on the sustainability of cork oak stands. A simulation approach. *Advances in Geocology*, 37:275–286.
- Ribeiro, N., Dias, S., Surový, P., Oliveira, A., 2006: Modelling Cork Oak Production in Portugal. Hasenauer, H. (ed.): *Tree Growth Models for Forest Management in Europe*. Kluwer Academic Publishers, Netherlands, p. 285–313.
- Ribeiro, N., Surový, P., Pinheiro, A., 2010: Adaptive management on sustainability of cork oak woodlands. In: B. Manos, K. Paparrizos, N. Matsatsinis and J. Papatthasiou (eds.): *Decision Support Systems in Agriculture, Food and the Environment: Trends, Applications and Advances*, IGI Global, p. 437–449.
- Ribeiro, N., Surový, P., 2011: Growth modeling in complex forest systems: CORKFITS a tree spatial growth model for cork oak woodlands. *FORMATH*, 10:263–278.
- Ribeiro, N., Surový, P., Yoshimoto, A., 2012: Optimal Regeneration Regime under Continuous Crown Cover Requirements in Cork Oak Woodlands. *FORMATH*, 11:83–102.
- Ribeiro, J., Ribeiro, N., Vaz, M., Dinis, C., Camilo-Alves, C., Poeiros, A. et al., 2021: Manual técnico de práticas silvícolas para a gestão sustentável em povoamentos de sobreiro e azinheira, Portugal, 126 p.
- Seidl, R., Thom, D., Kautz, M., Martin-Benito, D., Peltoniemi, M., Vacchiano, G. et al., 2017: Forest disturbances under climate change. *Nature Climate Change*, 7:395–402.

- Silva, M., 1996: Contributo para o estudo da qualidade da cortiça: Avaliação das relações existentes entre parâmetros definidores da sua qualidade. Provas de Aptidão Pedagógica e Capacidade Científica. Universidade de Trás-os-Montes e Alto Douro, Vila Real, 95 p.
- Silva, M., Marrafa S., Ribeiro, N., 2017: Avaliação da qualidade da cortiça em três descortiçamentos consecutivos: influência da árvore e da estrutura do povoamento. Livro de Resumos. 8º Congresso Florestal Nacional- Raízes do Futuro, Viana do Castelo, 179 p.
- Stock, S., 2009: MicroComputed Tomography- Methodology and Application. CRC Press, 331 p.
- Taylor, A., Plank, B., Standfest, G., Petutschnigg, A., 2013: Beech wood shrinkage observed at the micro-scale by a time series of X-ray computed tomographs ( $\mu$ XCT). *Holzforschung*, 67:201–205.

*Other sources*

FAO Soils Portal - <http://www.fao.org/soils-portal/en/>. Accessed in January 2021.

Portuguese Association of Cork. (APCOR) – [https://www.apcor.pt/wp-content/uploads/2019/12/boletim\\_estatistico\\_apcor\\_2019.pdf](https://www.apcor.pt/wp-content/uploads/2019/12/boletim_estatistico_apcor_2019.pdf). Accessed in December 2019.

PROF – Programa Regional de Ordenamento Florestal (2019) - <http://www2.icnf.pt/portal/florestas/profs/prof-em-vigor>. Accessed in October 2020.